

Crystallization Kinetics of Maleic Anhydride-Modified iPP Studied by POM

G. BOGOEVA-GACEVA,¹ B. MANGOVSKA,¹ E. MÄDER²

¹ Faculty of Technology & Metallurgy, University "St. Cyril and Methodius," R. Boskovic 16, Skopje, Macedonia

² Polymer Research Institute, Hohe Strasse 6, Dresden, Germany

Received 12 March 1999; accepted 27 May 1999

ABSTRACT: Melt nucleation and crystallization behavior of homo-isotactic polypropylene (homo-iPP), maleic anhydride (MAH)-grafted-iPP, and MAH-modified iPP, produced from iPP and a small amount of MAH-grafted-iPP, was investigated by polarizing optical microscopy (POM), at $T_c = 121\text{--}135^\circ\text{C}$. Nucleation processes at a given T_c were faster for modified PP as compared to neat iPP. The induction time for nucleation increased nonlinearly with increasing T_c and decreased for modified PP, probably as a result of promoted heterogeneous nucleation due to the presence of carbonyl groups of MAH-grafted-PP. The average spherulite sizes were decreased by modification, and the growth rate was enhanced in maleated PP and modified PP. The induction time approach was applied to the results obtained by POM to compare the tendency for heterogeneous nucleation of neat and MAH-modified PP. © 2000 John Wiley & Sons, Inc. *J Appl Polym Sci* 77: 3107–3118, 2000

Key words: polypropylene; maleic anhydride-modified; crystallization; polarizing optical microscopy

INTRODUCTION

The properties of semicrystalline thermoplastic polymers widely used in composite materials are closely related to the morphology developed during processing. Investigations of glass fiber/polypropylene (PP) composites have particularly shown that, under different consolidation conditions and additional annealing, a wide range of spherulitic morphology of isotactic polypropylene (iPP) can appear, differing in average spherulite size and overall crystallinity.^{1,2} As a result, different wetting of glass fibers is achieved and significant differences in interlaminar toughness,

mechanism of deformation, and crack propagation are found.²

The morphology and crystallization of iPP have been extensively studied and are reviewed in refs. 3 and 4. However, due to its nonpolar nature, the use of homo-iPP in composite materials, in which adhesion to and compatibility with the reinforcing fibers is an important factor, is limited. Modified PPs have recently been used in composite materials to obtain better interface-sensitive properties.⁵

In our previous publication, the influence of a small amount of maleic anhydride (MAH)-grafted PP on the kinetics of isothermal and nonisothermal crystallization of iPP was investigated by DSC.⁶ An improved nucleation ability of modified PP was shown to be a consequence of reduced critical dimensions of growing nuclei.^{6,7}

In this article, the morphology and crystallization kinetics of MAH-grafted iPP were investi-

Correspondence to: G. Bogoeva-Gaceva.
Contract grant sponsors: Ministry of Science of Macedonia; International Bureau of BMBF, Germany.

Journal of Applied Polymer Science, Vol. 77, 3107–3118 (2000)
© 2000 John Wiley & Sons, Inc.

gated by polarizing optical microscopy (POM) and the results are compared to those of unmodified iPP. Modified iPP was used for the production of warpknit composite preforms, consisting of continuous glass fibers, polymer film, and a polyester yarn loop system.⁸ In these materials, modified iPP was confirmed to improve the adhesion to glass fibers.⁹ According to the theory of nucleation control of spherulite growth,¹⁰ some energetic parameters of crystallization of PPs were calculated.

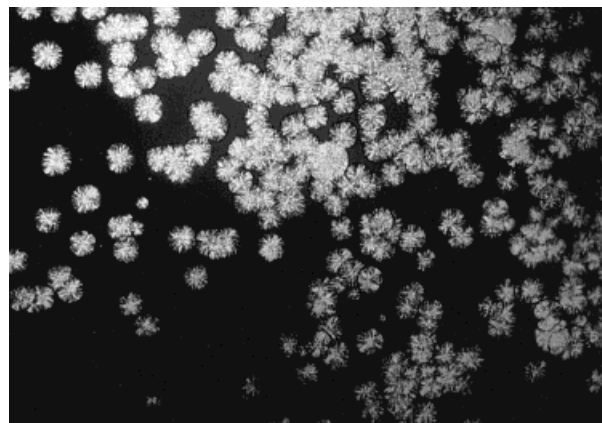
EXPERIMENTAL

The crystallization behavior of three PPs was investigated by POM. MAH-modified iPP (M-PP) with MFI = 36 g/10 min was produced by melt blending of commercial-grade Shell homo-iPP (PP-S) with a weight-average molecular weight of 158,500 (as determined by GPC) and a polydispersity index, M_w/M_n , of 6.36, with a commercial-grade modifier, MAH-grafted-PP [Polybond 3150, (PB)] with an M_w 90,000 and a grafting degree of 0.5% MAH.

Melt nucleation and crystallization of PPs were analyzed with POM (Leica Biomed) equipped with a hot-stage device (−20/350°C), temperature controller, and photcamera (Nikon-800). To avoid multiple scattering, extremely thin samples, with a nominal thickness of 0.02 mm, were prepared by melting the PP films between two microscopic slides (18 × 18 mm). For isothermal experiments, PP specimens were first heated to 205°C (about 20 K above their equilibrium melting temperature) and held there for 5 min to erase previous thermal history effects, and the melt was cooled to a predetermined crystallization temperature, $T_c = 121$ – 135 °C. Photographs were taken at appropriate time/temperature intervals. The radial growth rate of spherulites, G , at various T_c was determined using micrographs, from the slope of the curve radius versus time. For each T_c , at least three different trials were taken, and the standard deviation was $\pm 5\%$. For the analysis of the results obtained, the statistical PC program *Statgraf ver.2.2* was used. The induction time (t_i) for crystallization was determined by depolarization microscopy.

Energetics of Spherulite Growth

According to the theory of crystallization of polymers,¹⁰ the temperature dependence of the spherulite growth rate, G , is given by the relationship



(a)



(b)

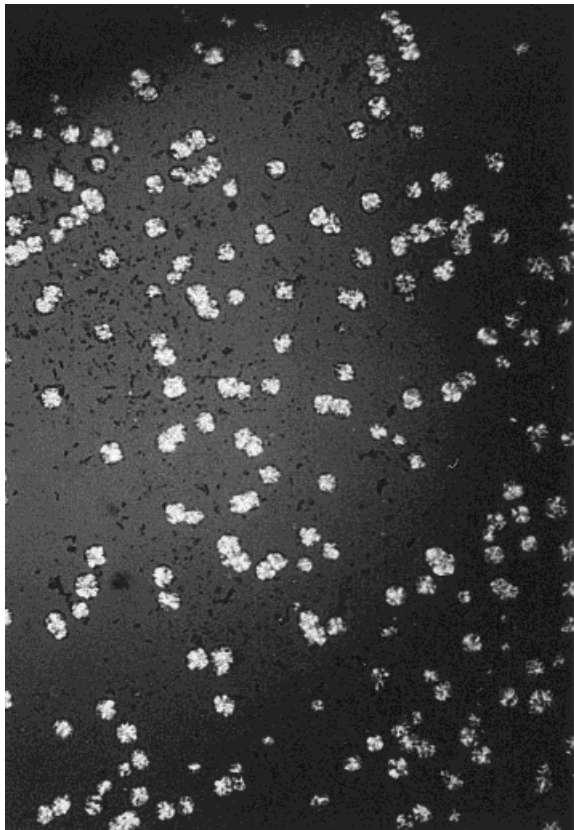
Figure 1 Optical micrographs of spherulitic morphology of PP-S crystallized at (a,b) $T_c = 121$ °C, (c–e) $T_c = 127$ °C, and (f–i) $T_c = 135$ °C.

$$\log G = \log G_0 - \frac{\Delta F^*}{2.3kT_c}$$

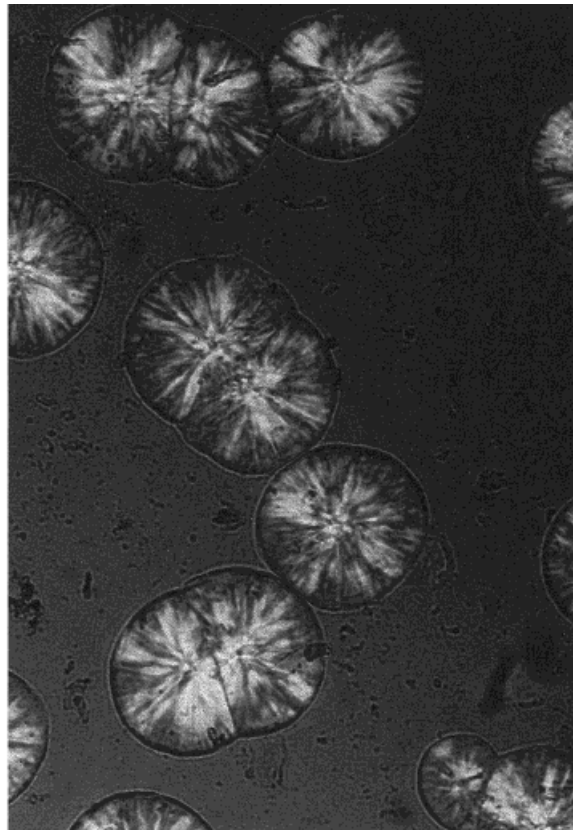
$$- \frac{4b_0\sigma\sigma_e T_m^0}{2.3k\Delta H_f\Delta T}$$

where G_0 is a constant dependent on the molecular parameters, but independent of the temperature; ΔF^* , the activation energy values for the transport processes of crystallization units at the liquid–solid interface; b_0 , the distance between two adjacent fold planes; the quantities σ and σ_e , the free energy of formation per unit area of lateral and fold surfaces, respectively; T_m^0 , the equilibrium melting temperature of the polymer; $\Delta T = T_m^0 - T_c$, the supercooling; and ΔH_f , the enthalpy of fusion per unit volume of the fully crystallized polymer.

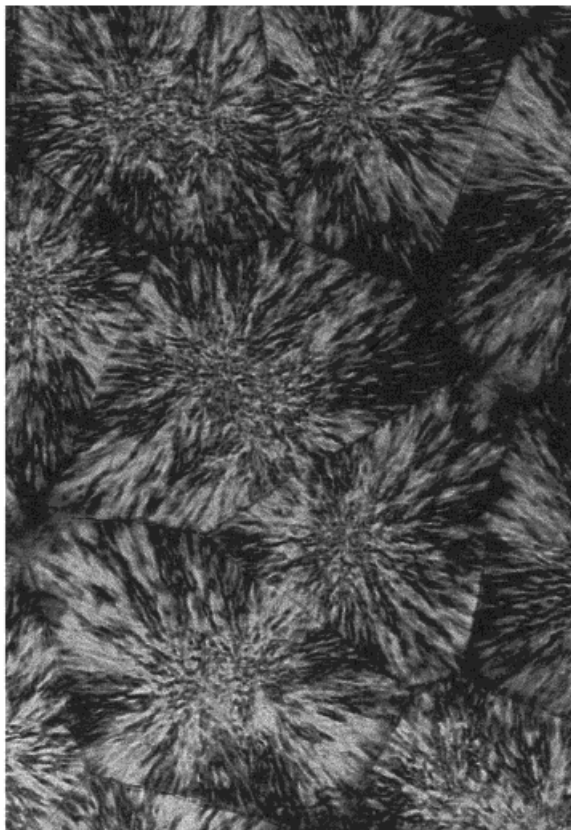
Linear regression analysis of the plot $\log G$ versus $1/T_c\sigma\sigma_e$ allows the determination of $\sigma\sigma_e$, where the slope of this straight line is equal to



(c)

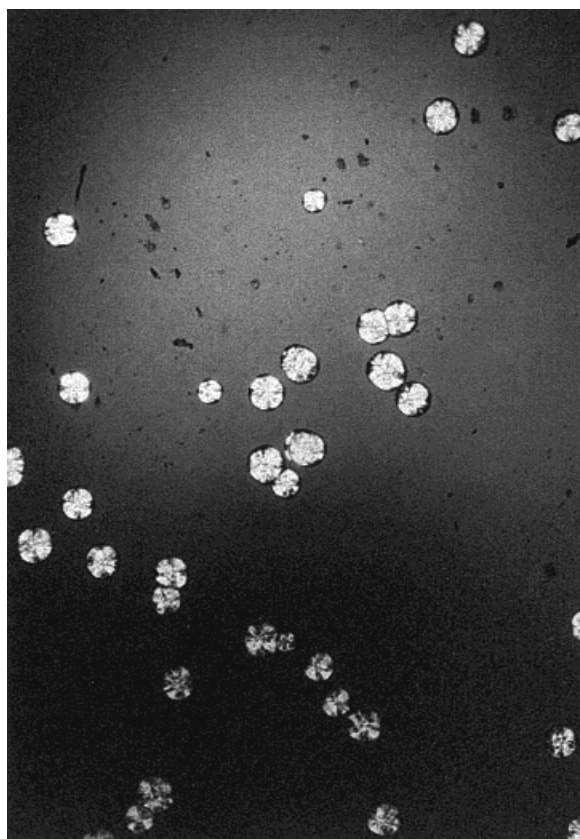


(d)

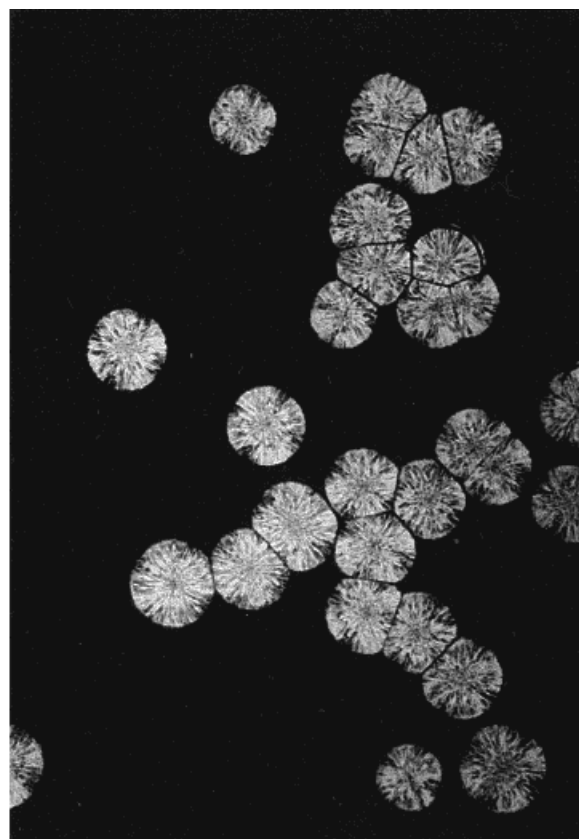


(e)

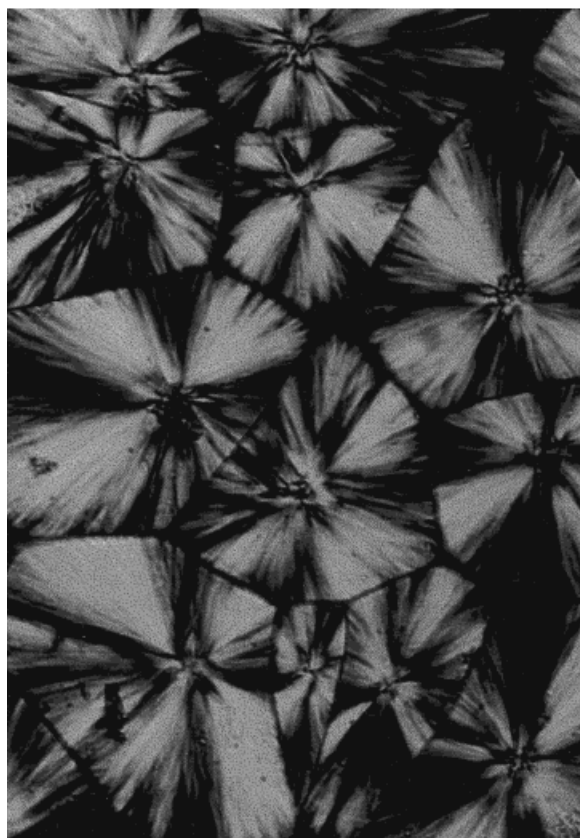
Figure 1 (Continued from the previous page)



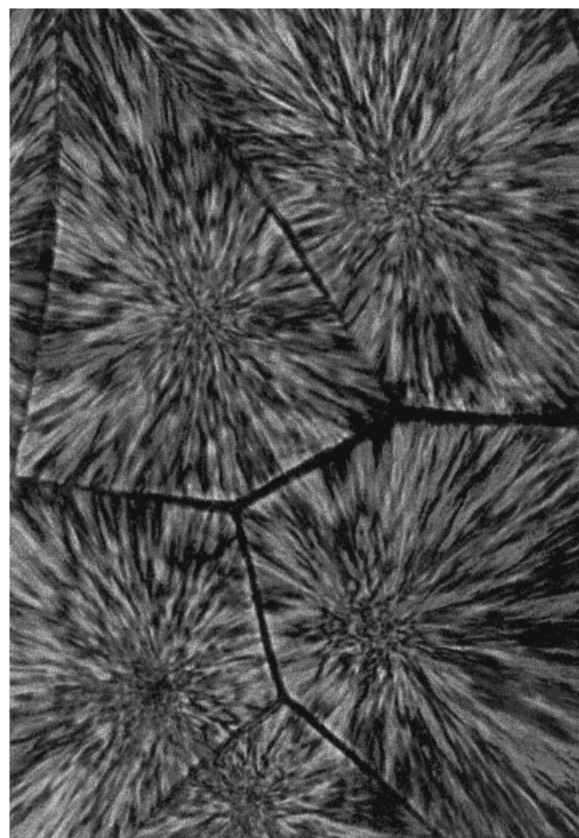
(f)



(g)



(h)



(i)

Figure 1 (Continued from the previous page)

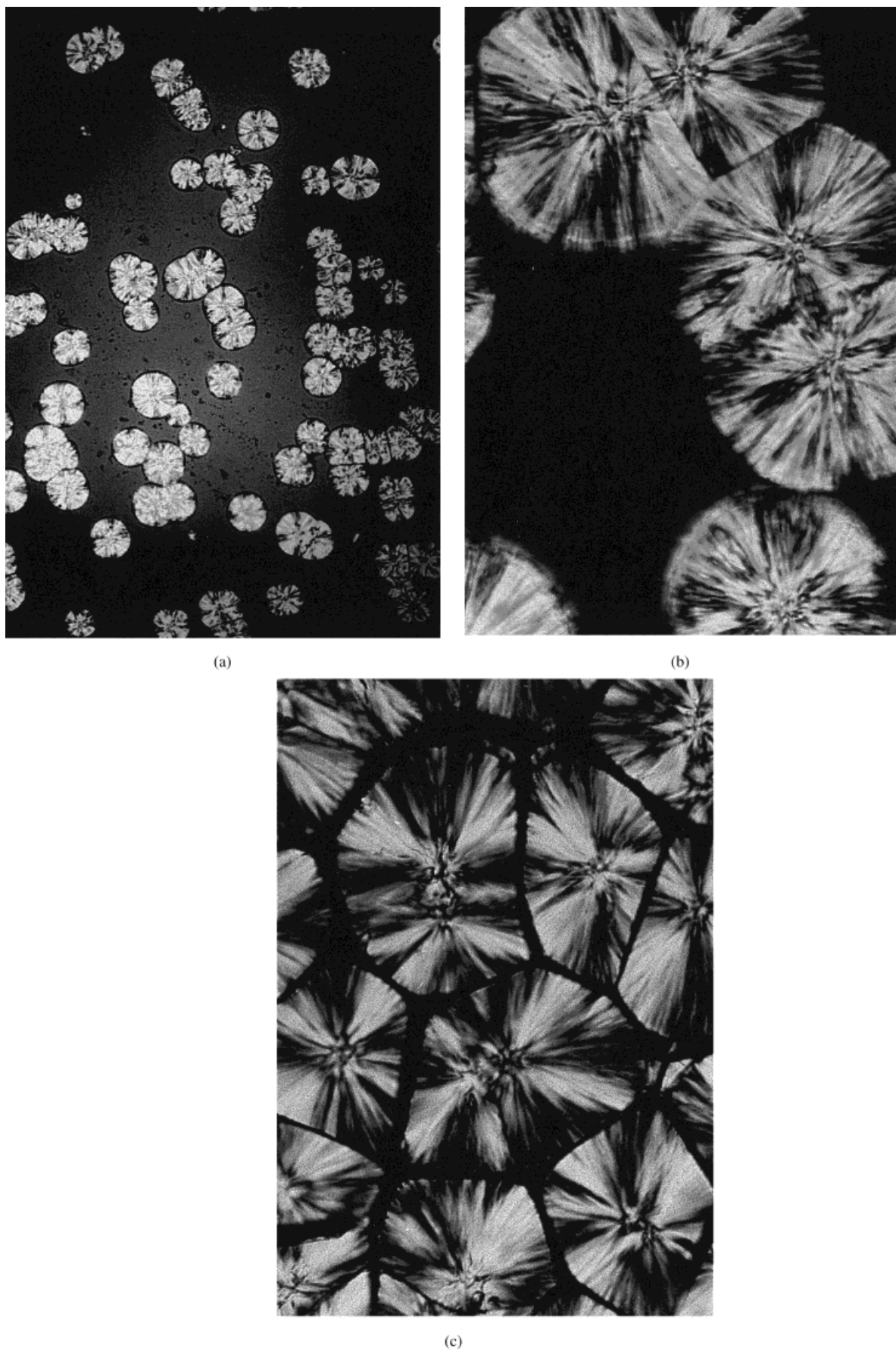


Figure 2 Optical micrographs of spherulitic morphology of M-PP crystallized at $T_c = 135^\circ\text{C}$ after (a) 150 min and (b) 190 min and (c) at the end of crystallization.

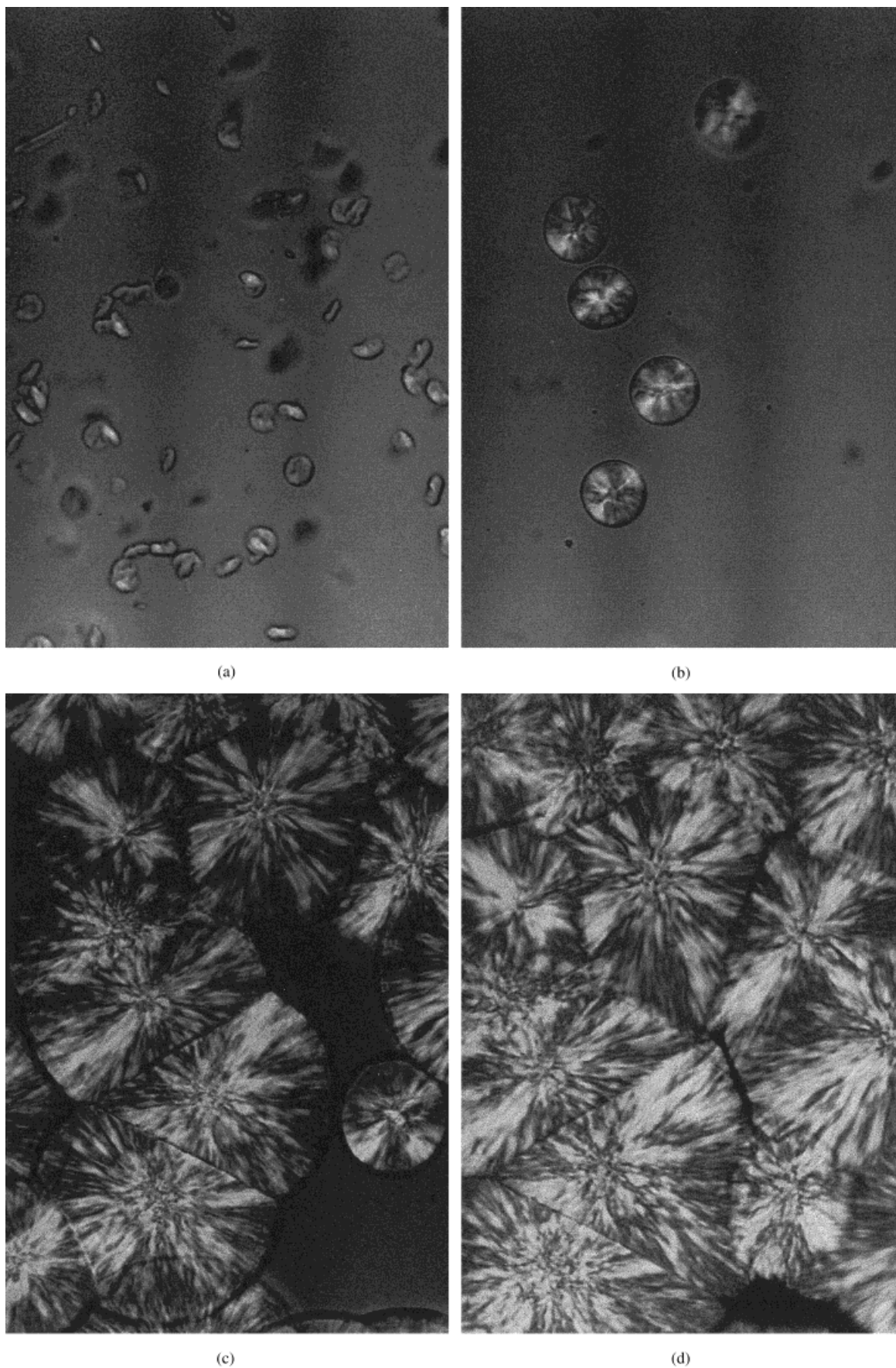
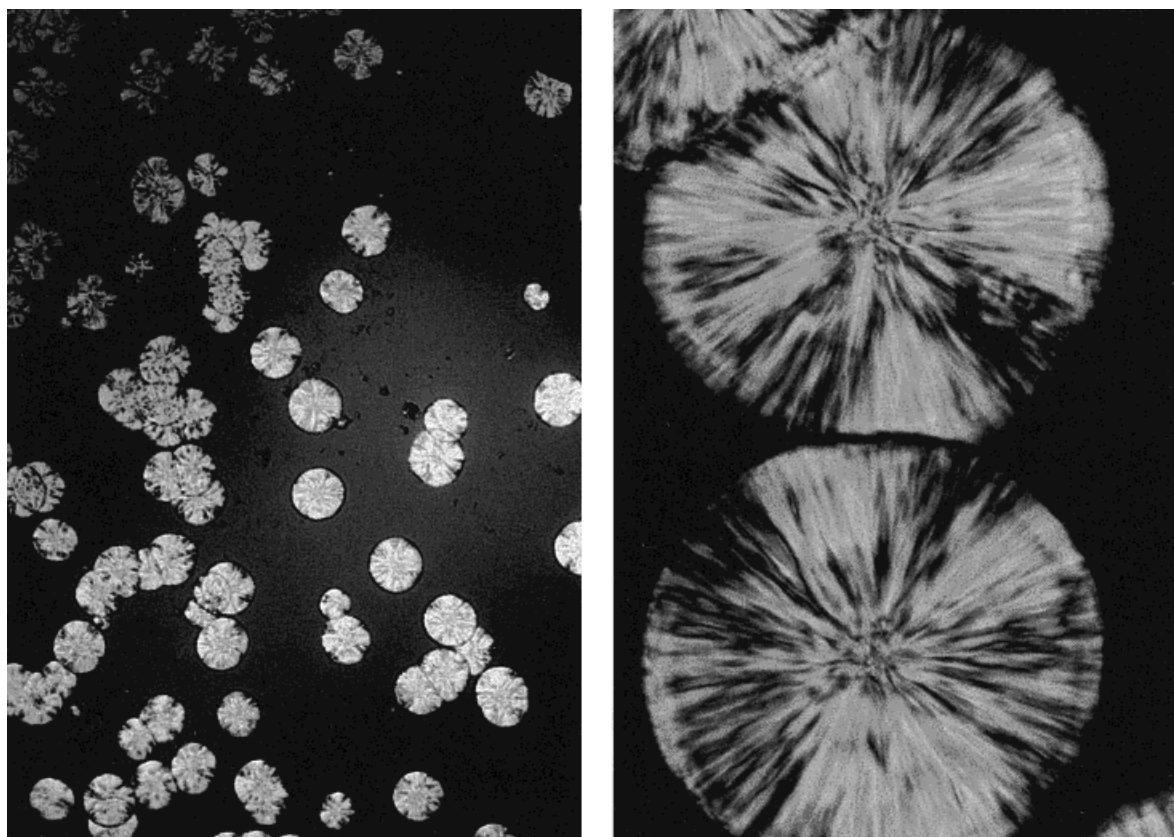
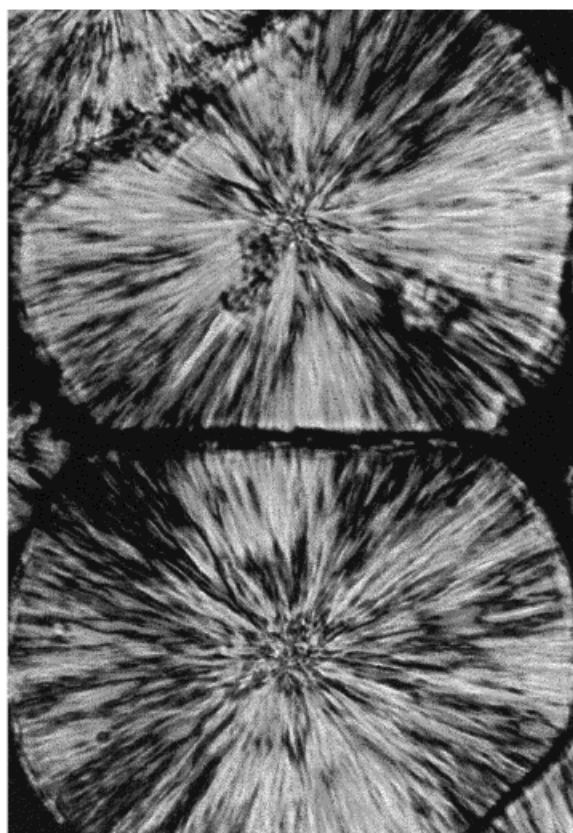


Figure 3 Optical micrographs of spherulitic morphology of PB crystallized at $T_c = 127^\circ\text{C}$: (a) 1 min; (b) 7 min; (c) 30 min; (d) 60 min, and at $T_c = 135^\circ\text{C}$: (e) 135 min; (f) 240 min; (g) 315 min.



(e)

(f)



(g)

Figure 3 (Continued from the previous page)

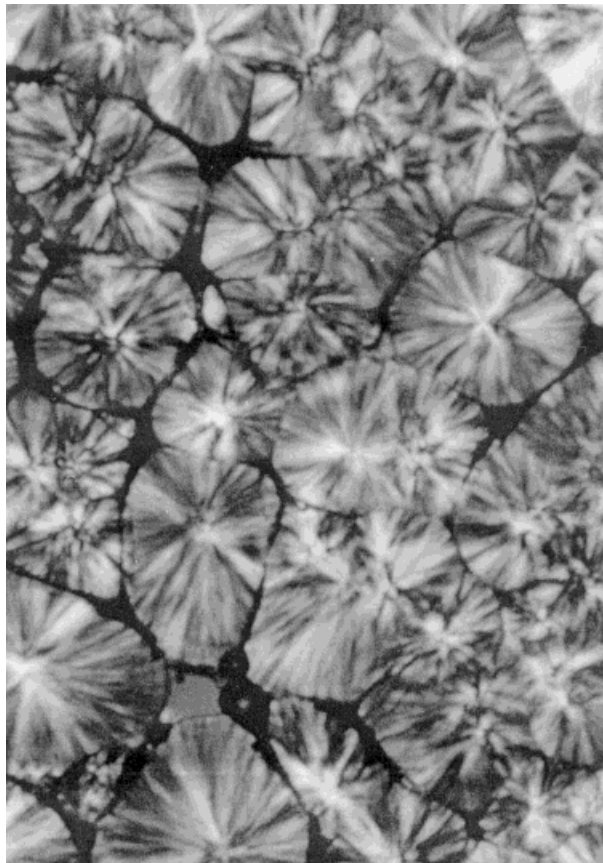


Figure 4 Spherulites of M-PP grown by isothermal crystallization at $T_c = 121^\circ\text{C}$. Note cracks, voids, and vacuum bubbles formed along the spherulite boundary.

$$-4b_0\sigma\sigma_e T_m^0 / 2,3 k\Delta H_f$$

Using the Williams, Landel, and Ferry relation,

$$\Delta F^* = C_1 T_c / (C_2 + T_c - T_g)$$

where C_1 is a constant = 17.2 kJ/mol for PP; C_2 , a constant = 51.5 K for PP; and T_g , the glass transition temperature (260 K). The temperature dependence of the activation energy for the transport processes of crystallization units at the liquid–solid interfaces was determined. According to the Gibbs–Thompson relation,

$$l = 2\sigma_e T_m^0 / \Delta H_f \Delta T$$

where σ_e is the crystal end (fold) surface energy [J/m^2]; T_m^0 , the equilibrium melting temperature [K]; l , the lamellar thickness [nm]; and ΔH_f , the heat of fusion per unit volume of the polymer with

100% crystallinity [J/m^3], the lamellar thickness, l , was determined.

RESULTS AND DISCUSSION

The micrographs shown in Figures 1–3 exhibit the behavior of PPs during isothermal crystallization at $T_c = 121$ – 135°C . It is apparent that the

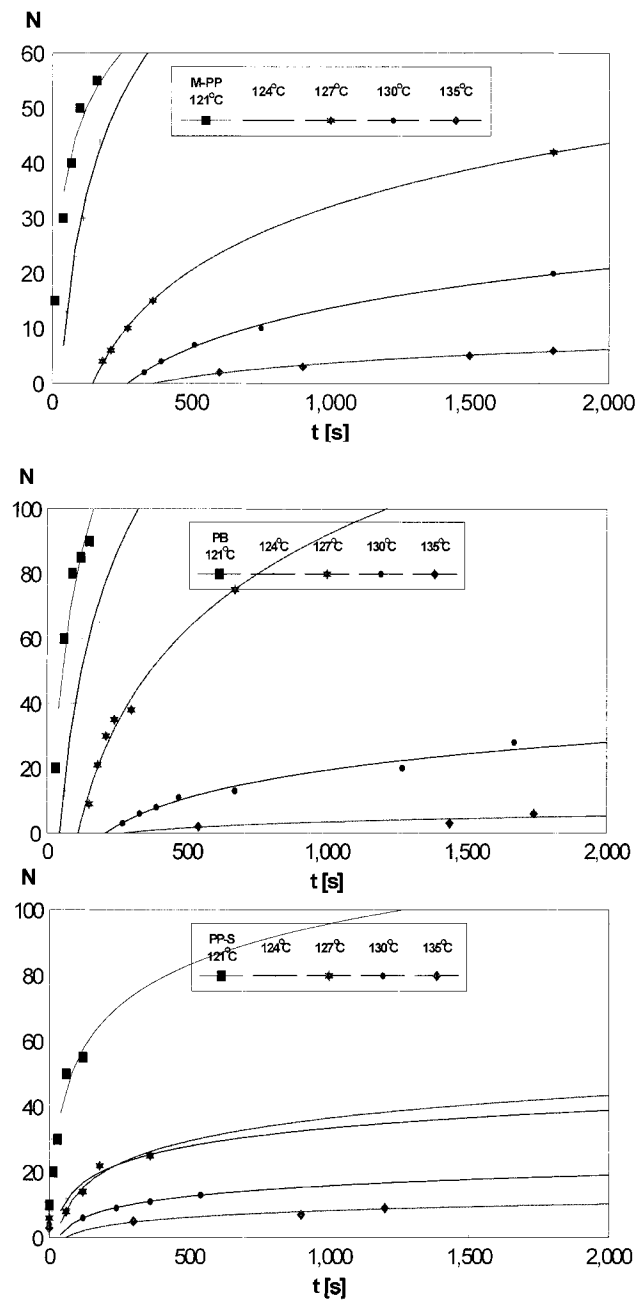


Figure 5 Number of spherulites (N) nucleated at different T_c versus time for M-PP, PB, and PP-S.

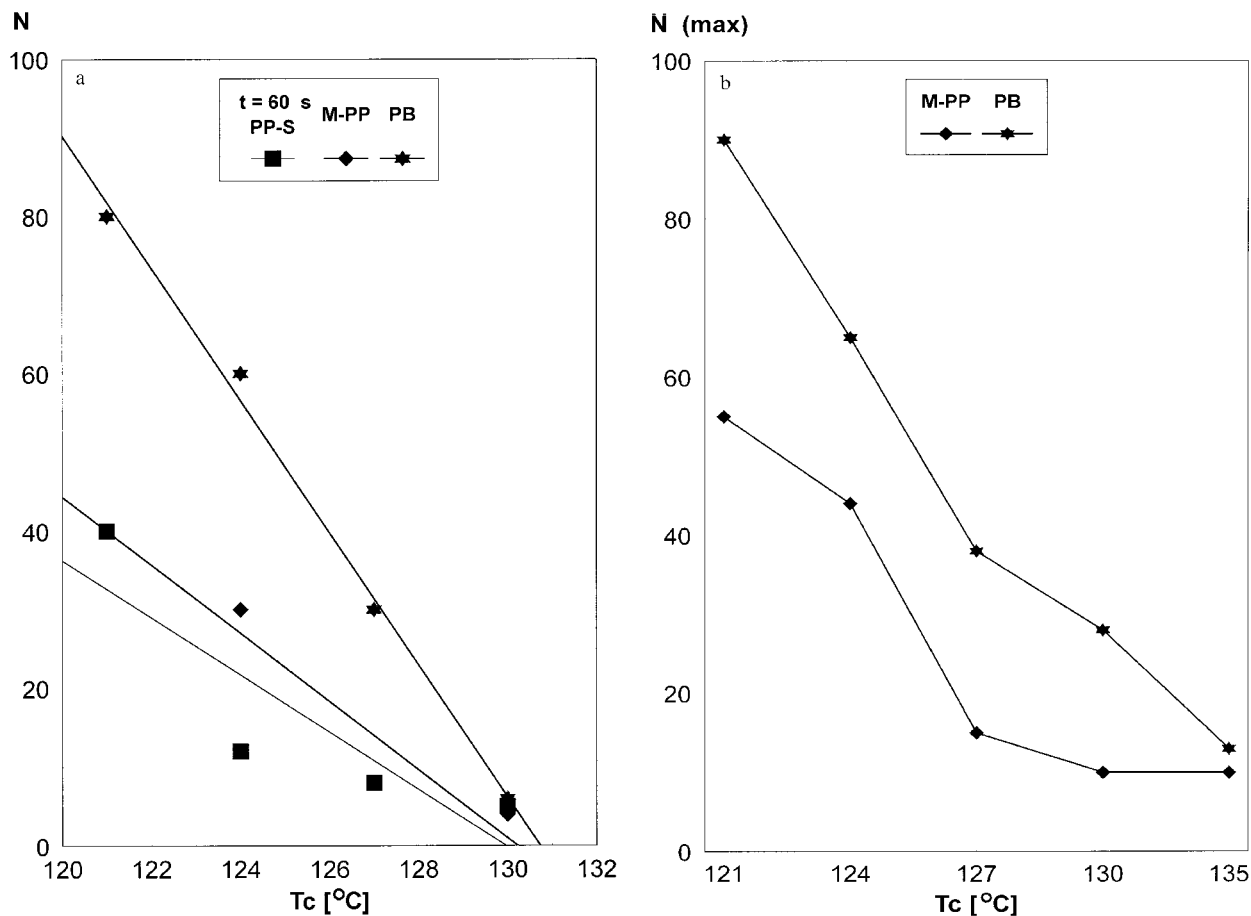


Figure 6 Nucleation density for M-PP, PP-S, and PB at different T_c (a) for the same crystallization time of 60 s and (b) at the final stage of the crystallization process.

spherulitic morphology of MAH-grafted-PP, as well as of the modified PP, is similar to that of neat PP, that is, it exhibits a typical Maltese cross extinction. However, the first visible nuclei of PB, appearing in the initial stage of growth, are bean-like [Fig. 3(a)].

The appearance of “cracked” spherulite boundaries after the impingement of neighboring spherulites, initially unhindered, causes formation of polygonal profiles, as shown in Figure 1(b,e,h). At higher T_c , a material-deficient boundary forms [see Figs. 1(i), 2(c), and 3(g)]. During the crystallization, cracks and voids, as well as some vacuum bubbles, are formed along the spherulite boundaries due to some contraction (see Fig. 4), representing weak sites in the polymer. Figure 4 shows also an irregular spherulitic texture arising from a higher population of primary nuclei, characteristic of low T_c . Most of the potential nuclei, developed at T_c higher than 121°C, are activated in the early stages of crys-

tallization, indicating predominant instantaneous nucleation. Sporadic-in-time nucleation was previously observed for PP-S at $T_c = 117$ – 121 °C. Change in the nucleation regime for both PP-S and M-PP in this T_c range was demonstrated by DSC analysis and the results were reported in our previous article.⁶

The number of spherulites (N) that appear at various T_c nucleated in bulk PPs is shown as a function of crystallization time in Figure 5. The number of spherulites significantly increases with decreasing T_c (increasing supercooling, $\Delta T = T_m^0 - T_c$) and the nucleation processes at a given T_c in PB and M-PP are obviously faster than in neat PP-S. Similar nucleation densities for all PPs are found only for T_c higher than 130°C. The differences in nucleation of PPs for the same crystallization time of 60 s and at the final stage of crystallization are illustrated in Figure 6. Generally, the finest morphology is observed for modified PP.

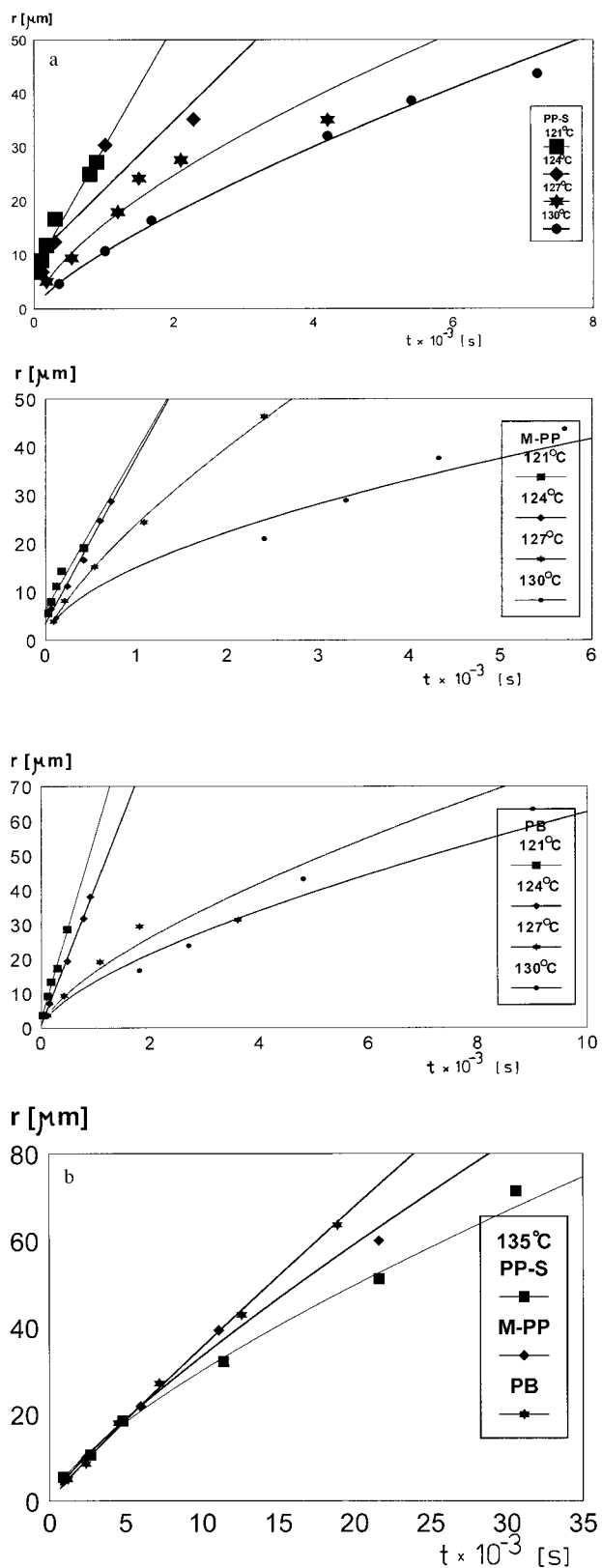


Figure 7 Radius of spherulites as a function of time at (a) $T_c = 121\text{--}130^\circ\text{C}$ and at (b) $T_c = 135^\circ\text{C}$ for PP-S, M-PP, and PB.

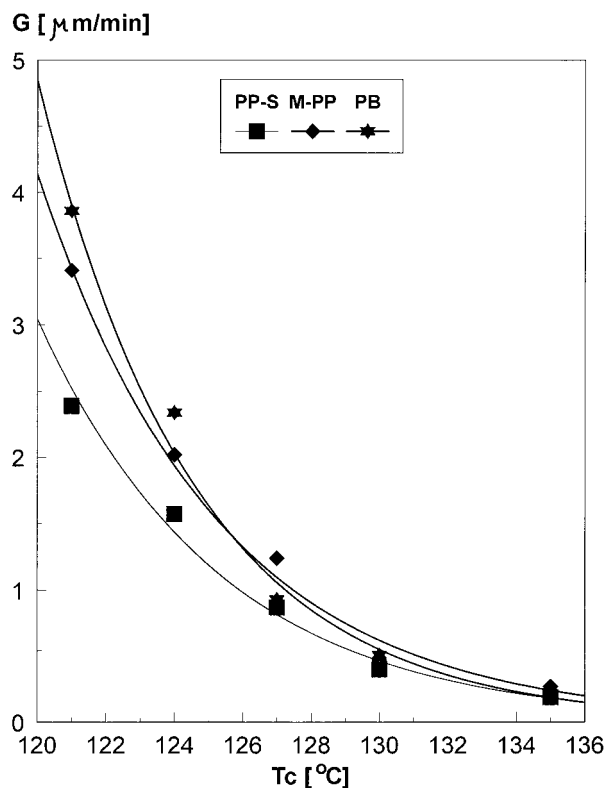


Figure 8 Plot of growth rate of spherulites (G) as a function of isothermal crystallization temperature, T_c , for PP-S, M-PP, and PB.

It is evident that T_c has a relevant influence on the nucleation processes up to 130°C . At higher T_c , insignificant variation in the number of spherulites was found for all investigated polymers after ~ 10 min of crystallization.

In the investigated range of T_c between 121 and 135°C , as confirmed by depolarization experiments, the induction time increases nonlinearly with increasing T_c . The lowest values for t_i were determined for M-PP (9 s/ 121°C ; 50 s/ 124°C ; 180 s/ 127°C ; 330 s/ 130°C ; 600 s/ 135°C), similar to those of PB, while the t_i for neat PP-S was almost twice as high. Induction time for crystallization depends on the ability of polymers for primary nucleation. The presence of carbonyl groups in PB and M-PP is believed to promote heterogeneous nucleation¹¹ and the reduction of t_i for both polymers might be attributed to this effect.

By reducing T_c , the average spherulite size decreases, as can be seen from Figure 7, apparently due to an increase in the average nucleation density. The average spherulite sizes were in the range of 20–180 μm and are obviously decreased by modification of iPP with PB. The spherulite

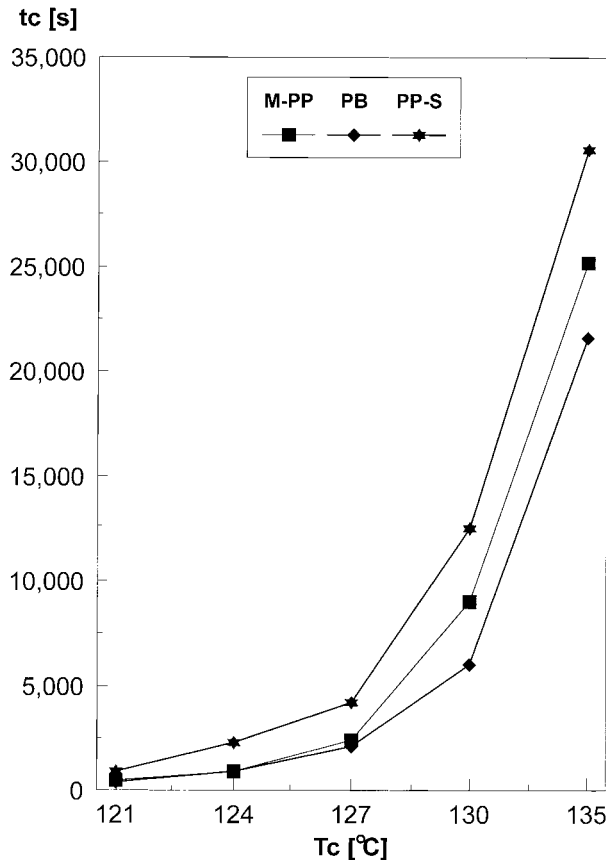


Figure 9 Overall time for crystallization (t_c) for M-PP, PB, and PP-S at different $T_c = 121$ – 135°C .

growth rates were measured from the dependence of the spherulite radii on time, prior to the impingement effects occurring, and the results are reported in Figure 8. The growth rate is enhanced in maleated PP (PB) and M-PP, and overall time for crystallization in the investigated range of the crystallization temperature was decreased by modification of PP with PB (see Fig. 9).

To study the early stages of heterogeneous crystallization, the theory of the induction time was developed,^{10, 11} according to which the induction time is a quantity that significantly reflects the mechanism of crystal nucleation. It was shown that the dependence of t_i versus $1/[T\Delta(T)^2]$ is linear (or close to) over the measured range of crystallization temperature (Fig. 10). This implies that the greatest consequence for the induction time determined is the formation of the first crystalline layer. A similar tendency is found for all PPs.

For the plots presented in Figure 10, values for T_m^0 previously obtained by DSC measurements were used.⁶ By regression analysis of the plot \log

G versus $1/T_c\sigma\sigma_e$, assuming $\sigma = 1.1 \times 10^{-5} \text{ J/cm}^2$, the crystal fold surface energy was calculated. A decreased value of $\sigma_e \approx 50 \text{ erg/cm}^2$ for M-PP was determined as compared to PP-S (75 erg/cm^2). $\sigma_e \approx 56 \text{ erg/cm}^2$ for PB was found. The obtained values do not exactly correspond to those obtained by DSC measurements,⁶ but the same trend of decreasing σ_e by modification with MAH-grafted PP is confirmed. A clear tendency of decreasing the lamellar thickness by reducing the T_c was also observed (Fig. 11), with lower values obtained for both PB and M-PP. The obtained results, together with decreased critical dimensions of a growing nucleus determined for M-PP by DSC,⁶ indicate significant changes in melt nucleation and spherulitic growth as a result of modification with MAH-grafted PP.

CONCLUSIONS

Melt nucleation and crystallization kinetics of iPP were significantly changed by modification with a small amount of MAH-grafted PP, although the

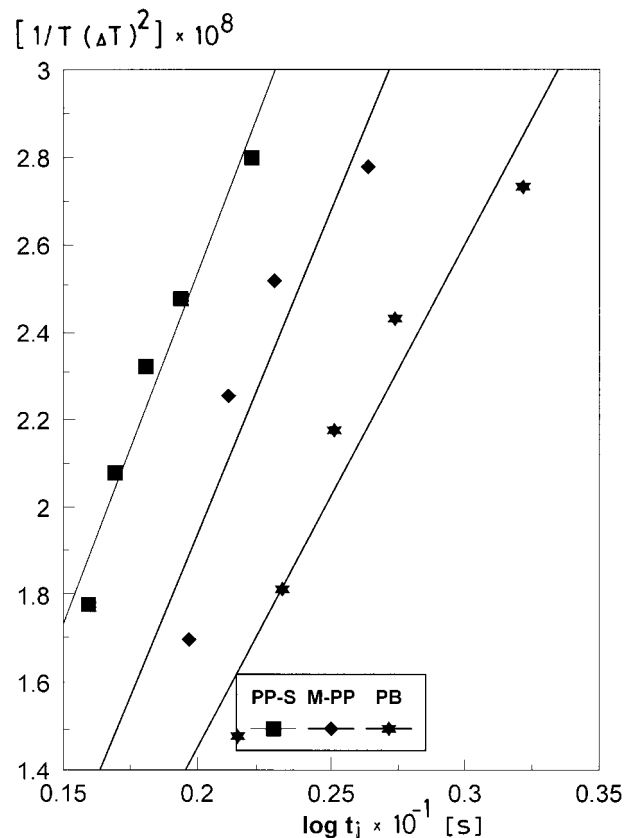


Figure 10 Dependence of t_i on $1/[T/(\Delta T)^2]$.

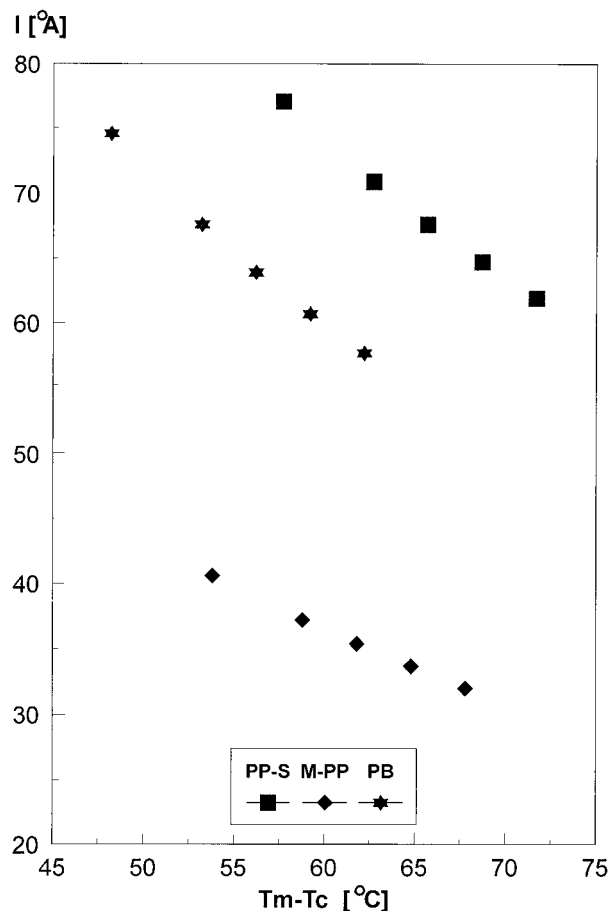


Figure 11 Dependence of lamellae thickness (l) for PP-S, M-PP, and PB on supercooling (ΔT).

spherulitic morphology of modified PP was similar to that of neat iPP. The changes in the nucleation processes and improved conditions for secondary nucleation found for modified PP by DSC

analysis⁶ were confirmed by the POM experiments in this article. Over the measured range of crystallization temperature (121–135°C), promoted heterogeneous nucleation was observed for MAH-modified iPP. A decreased value of σ_e was also determined as compared to neat iPP, and a lower value for lamellar thickness, decreased by reducing T_c , was found for modified iPP.

The results presented in this article are part of a bilateral project on thermoplastic-based composites, between the Faculty of Technology and Metallurgy in Skopje and the Institute of Polymer Research in Dresden, funded by the Ministry of Science of Macedonia and International Bureau of BMBF, Germany.

REFERENCES

1. Friedrich, K. *Prog Colloid Polym Sci* 1979, 66, 299.
2. Yan, L.; Friedrich, K. *Comp Sci Technol* 1993, 46, 187.
3. Varga, J. In *Polypropylene: Structure, Blends and Composites*; Karger-Kocsis, J., Ed.; Chapman & Hall: London, 1995; Vol. 1, Chapter 3, pp 56–115.
4. Clark, E. J.; Hoffman, J. D. *Macromolecules* 1984, 17, 878.
5. Mäder, E.; Skop-Cardarella, K. *TEXCOMP-3*, Aachen, Dec. 9–11, 1996.
6. Bogoeva-Gaceva, G.; Janeversuski, A.; Mäder, E. *J Adhes Sci Technol*, in press.
7. Janeversuski, A.; Bogoeva-Gaceva, G.; Mäder, E. *J Appl Polym Sci* 1999, 74, 239.
8. Mäder, E.; Skop-Cardarella, K. *Tech Text* 1996, 39, 124.
9. Mäder, E.; Jacobasch, H.-J.; Grundke, K.; Gietzelt, T. *Composites A* 1996, 27, 907.
10. Mandelkern, L. M. *Crystallization of Polymers*; McGraw-Hill: New York, 1964; Chapter 8.
11. Sathe, S. N.; Rao, G. S.; Devi, S. *J Appl Polym Sci* 1994, 53, 239.